

Article

LESO-Based Nonlinear Continuous Robust Stabilization Control of Underactuated TORA Systems

Yihao Wang ¹, Changzhong Pan ^{1,2,*} , Jinsen Xiao ³, Zhijing Li ¹ and Chenchen Cui ¹

¹ School of Information and Electrical Engineering, Hunan University of Science and Technology, Xiangtan 411201, China

² School of Automation, Guangdong University of Petrochemical Technology, Maoming 525000, China

³ Department of Mathematics, Guangdong University of Petrochemical Technology, Maoming 525000, China

* Correspondence: pancz@hnust.edu.cn

Abstract: In this paper, we consider the robust stabilization control problem of underactuated translational oscillator with a rotating actuator (TORA) system in the presence of unknown matched disturbances by employing continuous control inputs. A nonlinear continuous robust control approach is proposed by integrating the techniques of backstepping and linear extended state observer (LESO). Specifically, based on the backstepping design methodology, a hyperbolic tangent virtual control law is designed for the first subsystem of the cascaded TORA model, via which an integral chain error subsystem is subsequently constructed and the well-known LESO technique is easy to implement. Then, an LEO is designed to estimate the lumped matched disturbances in real-time, and the influence of the disturbances is compensated by augmenting the feedback controller with the disturbance estimation. The convergence and stability of the entire control system are rigorously proved by utilizing Lyapunov theory and LaSalle's invariance principle. Unlike some existing methods, the proposed controller is capable of generating robust and continuous control inputs, which guarantee that both the rotation and translation of TORA systems are stabilized at the origin simultaneously and smoothly, attenuating the influence of disturbances. Comparative simulation results are presented to demonstrate the effectiveness and superior control performance of the proposed method.

Keywords: underactuated mechanical systems; TORA; linear extended state observer (LESO); backstepping; stabilization



Citation: Wang, Y.; Pan, C.; Xiao, J.; Li, Z.; Cui, C. LESO-Based Nonlinear Continuous Robust Stabilization Control of Underactuated TORA Systems. *Actuators* **2022**, *11*, 220. <https://doi.org/10.3390/act11080220>

Academic Editor: Anyang Lu

Received: 18 July 2022

Accepted: 1 August 2022

Published: 4 August 2022

Publisher's Note: MDPI stays neutral with regard to jurisdictional claims in published maps and institutional affiliations.



Copyright: © 2022 by the authors. Licensee MDPI, Basel, Switzerland. This article is an open access article distributed under the terms and conditions of the Creative Commons Attribution (CC BY) license (<https://creativecommons.org/licenses/by/4.0/>).

1. Introduction

As a typical underactuated mechanical system [1–6], the translational oscillator with a rotating actuator (TORA) is composed of an unactuated translational trolley and an actuated rotational eccentric ball. It is thus featured by the characteristics of strong coupling and high nonlinearity, and often used as a benchmark system for the design and performance test of various nonlinear control algorithms [7–9]. In addition, the TORA system is also used in engineering as an active mass damper (AMD) for the active vibration suppression of large engineering systems [10–12], such as super high-rise buildings, long-span bridges, offshore floating wind turbines, etc. Furthermore, after some extensions, it can also be used to study the self-synchronized phenomenon of many mechanical systems [13,14], e.g., vibration sifters, hands-held vibration tools, vibration conveyors, etc. Therefore, the study of TORA systems is of great both theoretical and practical significance.

However, the stabilization control of TORA systems is very challenging because the trolley and the ball need to be stabilized simultaneously using only one actuator (control input). To achieve the stabilization objective, scholars have conducted extensive and in-depth research, and published many ambitious achievements in the past decades [15–22]. Roughly speaking, the obtained results can be classified into three categories: passivity-based control method, cascade-based control method, and other advanced/intelligent control method.

The passivity-based control method is to construct a control Lyapunov function according to the passivity property of TORA systems and design a controller by making the derivative of the Lyapunov function negative. In [23], the passivity property of TORA systems is analyzed, based on which an energy control Lyapunov function is constructed, and a simple state feedback controller is designed. In [24], a passivity-based adaptive controller with an online observation mechanism is proposed. In [25], an output feedback passive control method using energy shaping and damping injection techniques is presented. In [26], a virtual angular velocity feedback signal is constructed and an output feedback global stabilization control method is proposed. More recently, based on the virtual feedback signal, the authors in [27] improve the energy function and present an output feedback control method that can avoid the phenomenon of small ball circulation.

The cascade-based control method requires a coordinate transformation to convert the TORA model into a cascaded form. Due to the simple structure of the cascaded system, the recursive backstepping technique can be easily applied to design a stable controller. This merit makes the cascade-based method extremely favored by scholars. For example, the TORA systems in [28] are transformed into a strict feedback cascaded form by using a global coordinate transformation, and then an integral backstepping control method is proposed. In [29], the state variables are treated as virtual control inputs and a nonlinear backstepping controller is designed. Considering the drawback of “explosion of complexity” in the backstepping design procedure, a nonlinear dynamic surface controller is designed through a collocated partial feedback linearization and a global change of coordinates [30]. In [31], an adaptive backstepping control scheme is proposed and a TORA experimental implementation is introduced.

It should be noted that most of the above literature does not consider the influence of unknown disturbances. To deal with uncertainties, some advanced/intelligent control techniques such as equivalent input disturbance (EID) [32], adaptive control [33], fuzzy control [34], and neural network [31] have been employed to improve the robustness of TORA systems. However, these methods require either prior knowledge of the system model or online learning mechanisms, which make the developed control algorithms not only computationally expensive but also very difficult for engineering applications. Moreover, by combining the sliding mode control with the observer technique, many composite control schemes have been proposed. For example, two nonlinear disturbance observer-based sliding mode control approaches are presented in [35,36], where the nonlinear disturbance observers are used to estimate unknown external disturbances and compensate for their effects, and the sliding mode controllers are designed to stabilize the system. Nevertheless, the inherent chattering problem of the sliding mode control cannot be avoided, and the generated control signals are discontinuous.

Based upon the above analysis of the current research status of TORA systems, it is noted that there are still some open problems worthy of being further investigated, which are summarized as follows.

- (1) The control algorithms developed by the passivity-based control method are computationally simple but they are difficult to deal with unknown disturbances. In other words, when these controllers are applied for TORA systems in practice where unknown disturbances widely exist, the control performances of the controllers would deteriorate and even unstable results may be caused.
- (2) By introducing a coordinate transformation, the model of TORA systems becomes a relatively simple cascaded form, based on which the uncertain issue can be addressed by incorporating neural network/fuzzy system or sliding model control techniques. However, the transient control performances of the control system under these control schemes cannot be guaranteed as the corresponding inherent problems of computational complexity and chattering phenomenon cannot be avoided.

To tackle the above issues, this paper investigates the stabilization control problem of TORA systems suffering from unknown lumped matched disturbances. A novel continuous robust control approach is proposed by integrating the techniques of backstepping and

linear extended state observer (LESO). Firstly, the TORA dynamics with matched disturbances are transformed into a cascaded form through a series of coordinate transformations. Then, a hyperbolic tangent virtual control law is designed for the first subsystem of the cascaded model based on the backstepping design technique. After that, an integral chain error subsystem under the virtual control law is constructed, and an LESO is designed to estimate the unknown disturbances. Based on the estimation of the LESO, a nonlinear state feedback control law with a compensation term is derived subsequently. Finally, the stability of the resulting control system is proved by using strict mathematical analysis, and numerical simulations with comparisons to the existing method are conducted to demonstrate the effectiveness and superiority of the proposed method.

To sum up, the main contributions and novel features of this paper are underlined as follows.

- (1) By borrowing the idea from the backstepping methodology, a hyperbolic tangent virtual control law is designed to obtain an integral chain error subsystem, which makes the well-known LESO technique easy to implement for the control design of TORA systems.
- (2) By employing the LESO, the unknown lumped matched disturbances are accurately estimated and timely compensated by augmenting the feedback controller with the estimate of disturbances, which guarantees the controller a strong robustness against disturbances.
- (3) Unlike some existing intelligent or sliding model control methods, the developed controller can generate robust and continuous control inputs to stabilize the rotation and translation of TORA systems smoothly and efficiently, without any learning mechanisms.

The remainder of this paper is organized as follows. The dynamics of an underactuated TORA system and the corresponding control problem are presented in Section 2. In Section 3, the detailed designs of the control approach, including a virtual control law, a LESO, and a continuous nonlinear feedback control law are described. The stability analysis of the closed-loop system is given in Section 4. Simulation results with comparisons are shown in Section 5. The main concluding remarks are ended in Section 6.

2. Control Problem Formulation

This paper focuses on the stabilization control problem of an underactuated horizontal TORA system subject to unknown matched disturbances. The physical structure of the TORA system is shown in Figure 1, and the physical parameters are given in Table 1.

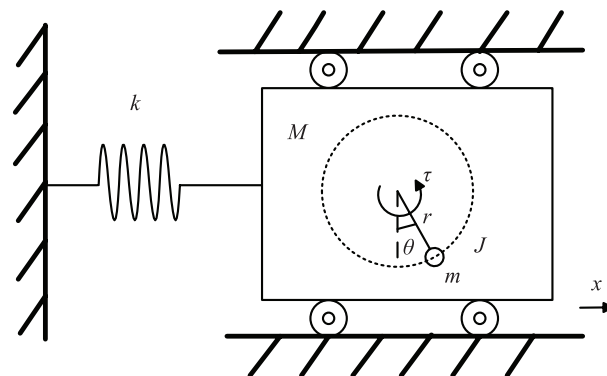


Figure 1. Physical structure diagram of an underactuated horizontal TORA system.

According to Euler–Lagrange modeling method, the dynamic equations of the TORA system are mathematically obtained as [18]

$$\begin{cases} (M + m)\ddot{x} + mr\ddot{\theta} \cos \theta - mr\dot{\theta}^2 \sin \theta + kx = 0 \\ mr\ddot{x} \cos \theta + (mr^2 + J)\ddot{\theta} = \tau + d \end{cases} \quad (1)$$

where d denotes the sum of matched unknown disturbances. In practice, it is mainly determined by the friction term and the bounded external disturbances.

Table 1. Physical parameters and variables of the TORA system.

Parameters/Variables	Meaning	Unit
M	Mass of the translational trolley	kg
m	Mass of the rotational ball	kg
k	Stiffness coefficient of the spring	N/m
r	Rotational radius of the ball	m
x	Translational displacement of the trolley	m
θ	Rotational angle of the ball with respect to the vertical position	rad
J	Moment of inertia of the ball	kg · m ²
τ	Control torque applied on the ball	N · m

To facilitate the controller design and stability analysis, the following dimensionless auxiliary variables are introduced [17]:

$$\chi = \sqrt{\frac{M+m}{mr^2+J}}x, u = \frac{M+m}{k(mr^2+J)}\tau, \varepsilon = \frac{mr}{\sqrt{(mr^2+J)(M+m)}} \tag{2}$$

$$T = \sqrt{\frac{k}{M+m}}t, d_\tau = \frac{M+m}{k(mr^2+J)}d$$

where T represents the dimensionless time, χ is the dimensionless trolley displacement, u is the dimensionless control torque, and d_τ is the dimensionless lumped disturbance. For the simplicity of notation, unless otherwise specified, the expression of “time” herein stands for “the dimensionless time”.

According to the introduced dimensionless variables in (2), the dynamics (1) can be rewritten as

$$\begin{cases} \ddot{\chi} + \chi + \varepsilon(\ddot{\theta} \cos \theta - \dot{\theta}^2 \sin \theta) = 0 \\ \ddot{\theta} + \varepsilon\dot{\chi} \cos \theta = u + d_\tau \end{cases} \tag{3}$$

Define the following variable transformations [35]:

$$\xi_1 = \chi + \varepsilon \sin \theta, \xi_2 = \dot{\chi} + \varepsilon \dot{\theta} \cos \theta, y_1 = \theta, y_2 = \dot{\theta} \tag{4}$$

then the dynamic Equation (3) is rearranged as the following cascaded form:

$$\begin{cases} \dot{\xi}_1 = \xi_2 \\ \dot{\xi}_2 = -\xi_1 + \varepsilon \sin y_1 \end{cases} \tag{5}$$

$$\begin{cases} \dot{y}_1 = y_2 \\ \dot{y}_2 = \frac{\delta_1 + u + d_\tau}{\delta_2} \end{cases} \tag{6}$$

where

$$\begin{aligned} \delta_1 &= \varepsilon \cos y_1 [\xi_1 - (1 + y_2^2)\varepsilon \sin y_1] \\ \delta_2 &= 1 - \varepsilon^2 \cos^2 y_1 \end{aligned} \tag{7}$$

Note that $0 < \varepsilon < 1$, which indicates that $\delta_2 > 0$.

Therefore, the control problem of this paper is formulated as: Consider the TORA system described by Equations (5) and (6) in the presence of unknown matched disturbances. Design a proper controller u such that the TORA system is stabilized at the equilibrium point, that is,

$$\lim_{T \rightarrow \infty} [\xi_1 \quad \xi_2 \quad y_1 \quad y_2]^T = [0 \quad 0 \quad 0 \quad 0]^T \tag{8}$$

which, applying the transformations (2) and (4), is equivalent to

$$\lim_{T \rightarrow \infty} [\chi \quad \dot{\chi} \quad \theta \quad \dot{\theta}]^\top = [0 \quad 0 \quad 0 \quad 0]^\top \quad (9)$$

and

$$\lim_{T \rightarrow \infty} [x \quad \dot{x} \quad \theta \quad \dot{\theta}]^\top = [0 \quad 0 \quad 0 \quad 0]^\top \quad (10)$$

3. LESO-Based Backstepping Controller Design

In this section, to achieve the above control objective, a virtual control law is firstly designed for the subsystem (5) based on the methodology of backstepping, and then a linear extended state observer (LESO) is employed to estimate the unknown disturbances based on which a state feedback control law is finally developed.

3.1. Virtual Control Law

Motivated by the control idea of backstepping methodology, the variable y_1 can be considered as the control input of subsystem (5), and a virtual control law defined as y_{1d} is designed to stabilize ζ_1 and ζ_2 . To this end, the following control Lyapunov function is constructed:

$$V_1 = \frac{1}{2}\zeta_1^2 + \frac{1}{2}\zeta_2^2 \quad (11)$$

Taking the time derivative of (11) along (5) yields

$$\dot{V}_1 = \zeta_1\dot{\zeta}_1 + \zeta_2\dot{\zeta}_2 = \zeta_1\zeta_2 + \zeta_2(-\zeta_1 + \varepsilon \sin y_{1d}) = \zeta_2\varepsilon \sin y_{1d} \quad (12)$$

In order to make \dot{V}_1 negative, the virtual control law y_{1d} is designed as

$$y_{1d} = -\tanh(\alpha\zeta_2) \quad (13)$$

where α is a positive constant. The deviation between y_1 and y_{1d} is defined as

$$e_1 = y_1 - y_{1d} = y_1 + \tanh(\alpha\zeta_2) \quad (14)$$

Calculating the first and second-time derivatives of (14) yields

$$\begin{cases} \dot{e}_1 = e_2 \\ \ddot{e}_1 = \frac{\delta_1 + u + d_\tau}{\delta_2} - \dot{y}_{1d} \end{cases} \quad (15)$$

where \dot{y}_{1d} and \ddot{y}_{1d} can be expressed explicitly as

$$\begin{aligned} \dot{y}_{1d} &= \alpha(\zeta_1 - \varepsilon \sin y_1) \left(1 - \tanh^2(\alpha\zeta_2)\right) \\ \ddot{y}_{1d} &= \left(\alpha(\zeta_2 - \varepsilon y_2 \cos y_1) - 2\alpha^2(\zeta_1 - \tanh(\alpha\zeta_2))\right) \left(1 - \tanh^2(\alpha\zeta_2)\right) \end{aligned} \quad (16)$$

Letting $[e_2 \quad \dot{e}_2]^\top = [\dot{e}_1 \quad \ddot{e}_1]^\top$ and using (14)–(16), the cascaded model (5) and (6) of the TORA system can be written as

$$\begin{cases} \dot{\zeta}_1 = \zeta_2 \\ \dot{\zeta}_2 = -\zeta_1 + \varepsilon \sin(e_1 + y_{1d}) \end{cases} \quad (17)$$

and

$$\begin{cases} \dot{e}_1 = e_2 \\ \dot{e}_2 = \frac{\delta_1 + u + d_\tau}{\delta_2} - \dot{y}_{1d} \end{cases} \quad (18)$$

Remark 1. Note that by designing the virtual control law (13), a simple integral chain error subsystem is obtained as (18). It will prove in Section 4 that if a proper controller u is designed such that the error subsystem (18) is stabilized at the origin, then the subsystem (17) is also stabilized at the origin; that is, the control objective is realized. However, there exists an unknown matched disturbance d_τ in Equation (18), which makes the controller design quite difficult. To address this problem, a linear extended state observer (LESO) is employed to estimate the unknown disturbance in real-time and the estimation value is fed back to the controller to compensate for its effect. This is the basic idea of the proposed control method.

3.2. Linear Extended State Observer (LESO)

As a crucial part of the active disturbance rejection control (ADRC), extended state observer (ESO) is an effective and practical disturbance estimation and attenuation approach [37,38]. To make the controller easy to implement, a linear ESO (LESO) is proposed in [39], where nonlinear gains are replaced with linear ones. Due to this promising feature, LESO has already been widely applied in many engineering control systems.

To implement the LESO technique, the subsystem (18) is further rearranged as

$$\begin{cases} \dot{e}_1 = e_2 \\ \dot{e}_2 = \frac{\delta_1}{\delta_2} + \frac{1}{\delta_2}u - \ddot{y}_{1d} + d_n \\ \dot{d}_n = \frac{d_\tau}{\delta_2} \end{cases} \quad (19)$$

Letting $[z_1 \ z_2 \ z_3]^\top = [e_1 \ e_2 \ d_n]^\top$, Equation (19) is written as

$$\begin{cases} \dot{z}_1 = z_2 \\ \dot{z}_2 = \frac{\delta_1}{\delta_2} + \frac{1}{\delta_2}u - \ddot{y}_{1d} + z_3 \\ \dot{z}_3 = h \end{cases} \quad (20)$$

where h is the change rate of the lumped disturbance, i.e., $h = \dot{d}_n$ and it is assumed to be an unknown but bounded function. Then, the LESO of the system (20) is designed as

$$\begin{cases} e_{s1} = \hat{z}_1 - z_1 \\ \dot{\hat{z}}_1 = \hat{z}_2 - \beta_1 e_{s1} \\ \dot{\hat{z}}_2 = \hat{z}_3 - \beta_2 e_{s1} + \frac{\delta_1}{\delta_2} + \frac{u}{\delta_2} - \ddot{y}_{1d} \\ \dot{\hat{z}}_3 = -\beta_3 e_{s1} \end{cases} \quad (21)$$

where $\hat{z}_i (i = 1, 2, 3)$ are the estimate values of z_i , and the quantities $\beta_i (i = 1, 2, 3)$ are the observer gains, which, for the sake of stability, should be chosen such that

$$s^3 + \beta_1 s^2 + \beta_2 s + \beta_3 = (s + \omega_0)^3 \quad (22)$$

where $\omega_0 > 0$ is the adjustable error feedback gain, which is also called the bandwidth of the LESO. From (22), the gains of the LESO are selected as

$$[\beta_1 \ \beta_2 \ \beta_3]^\top = [3\omega_0 \ 3\omega_0^2 \ \omega_0^3]^\top \quad (23)$$

Combining (20) and (21), the error dynamics of the LESO is obtained as

$$\begin{cases} \dot{e}_{s1} = e_{s2} - \beta_1 e_{s1} \\ \dot{e}_{s2} = e_{s3} - \beta_2 e_{s1} \\ \dot{e}_{s3} = -h - \beta_3 e_{s1} \end{cases} \quad (24)$$

where $e_{si} = \hat{z}_i - z_i (i = 1, 2, 3)$ are the estimation errors.

3.3. Continuous Nonlinear Feedback Control Law

Based on the virtual control law (13) and the LESO (21), we are ready to design a feedback control law to stabilize the subsystem (18), which is equivalent to (20). To this end, the following control Lyapunov function is constructed:

$$V_2 = \frac{1}{2}z_1^2 + \frac{1}{2}z_2^2 \tag{25}$$

Taking the time derivative of (25) along (20) yields

$$\dot{V}_2 = z_1z_2 + z_2\dot{z}_2 = z_2 \left[z_1 + \frac{\delta_1}{\delta_2} + \frac{1}{\delta_2}u - \ddot{y}_{1d} + z_3 \right] \tag{26}$$

To make \dot{V}_2 negative, a nonlinear state feedback control law is designed as

$$u = - \left(k_1z_2 + z_1 + \hat{z}_3 + \frac{\delta_1}{\delta_2} - \ddot{y}_{1d} \right) \delta_2 \tag{27}$$

where $k_1 > 0$ is the control gain.

So far, the designed controller is made up of the virtual control law (13), the LESO (21), and the nonlinear feedback control law (27). The block diagram of the control system is shown in Figure 2.

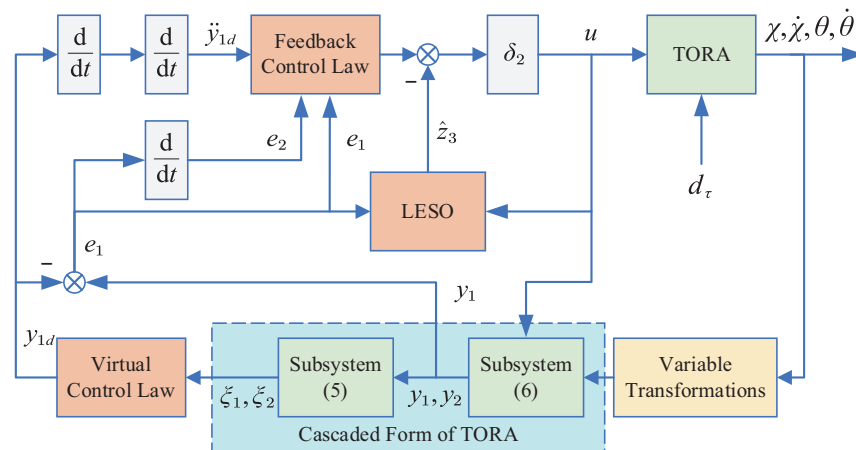


Figure 2. Block diagram of the closed-loop TORA control system.

Remark 2. It can be seen from Equation (27) and Figure 2 that the structure of the proposed controller, compared with other methods like [17,35], is relatively simple, which only needs the state feedback signals z_1, z_2 , the estimate \hat{z}_3 , and the virtual control signal \dot{y}_{1d} . The estimate signal \hat{z}_3 comes from the LESO, which is used to timely compensate for the effect of the unknown disturbance d_τ . In addition, unlike the methods using sliding mode control (SMC), where the inherent chattering phenomenon cannot be eliminated, the proposed controller can generate a continuous control signal, which would achieve a smooth and robust control performance. This merit will be further verified through comparison simulation studies in Section 5.

4. Stability Analysis

In this section, the convergence of the estimation errors of the proposed LESO (21) is first analyzed from the error dynamics (25) using Lyapunov stability theory. Then, the stability of the resulting TORA control system (5) and (6) under the virtual control law (13), the feedback control law (27) and the LESO (21) is rigorously proved by using LaSalle’s invariance principle.

To facilitate the stability analysis, the following assumptions are made for the TORA system.

Assumption 1 ([35]). *The first order derivatives of the unknown matched disturbances d_τ and d_n are bounded, i.e.,*

$$\|\dot{d}_\tau\| \leq \sigma_p, \quad \|h\| = \|\dot{d}_n\| \leq \sigma_{es} \tag{28}$$

where σ_p and σ_{es} are positive constants.

Theorem 1. *Consider the proposed LESO (21) for subsystem (20), if Assumption 1 holds, then the estimation error of the LESO is bounded, and satisfies*

$$\lim_{\omega_o \rightarrow \infty, T \rightarrow \infty} \|e_s\| = 0 \tag{29}$$

where $e_s = [e_{s1} \quad e_{s2} \quad e_{s3}]^\top$.

Proof. Letting $\eta_i = \frac{e_{si}}{\omega_o^i}$ ($i = 1, 2, 3$), Equation (24) is written as

$$\begin{cases} \dot{\eta}_1 = \omega_o(\eta_2 - 3\eta_1) \\ \dot{\eta}_2 = \omega_o(\eta_3 - 3\eta_1) \\ \dot{\eta}_3 = \omega_o\left(-\frac{h}{\omega_o^4} - \eta_1\right) \end{cases} \tag{30}$$

Rewriting Equation (30) into a compact form obtains

$$\dot{\eta} = \omega_o A_\eta \eta + B_\eta \frac{h}{\omega_o^3} \tag{31}$$

where $\eta = [\eta_1 \quad \eta_2 \quad \eta_3]^\top$,

$$A_\eta = \begin{bmatrix} -3 & 1 & 0 \\ -3 & 0 & 1 \\ -1 & 0 & 0 \end{bmatrix}, \quad B_\eta = \begin{bmatrix} 0 \\ 0 \\ -1 \end{bmatrix} \tag{32}$$

It can be seen from Equations (22) and (31) that, for any $\omega_o > 0$, A_η is obtained as (32), which is a Hurwitz matrix, thus select a Lyapunov function as

$$V(\eta) = \eta^\top P_\eta \eta \tag{33}$$

where P_η is a positive definite symmetric matrix and satisfies $A_\eta^\top P_\eta + P_\eta A_\eta = -Q_\eta$. Taking the time derivative of $V(\eta)$ along (32) and using Assumption 1 yields

$$\dot{V}(\eta) = -\omega_o \eta^\top Q_\eta \eta + 2\eta^\top P_\eta B_\eta \frac{h}{\omega_o^3} \leq -\omega_o \lambda_{\min}(Q_\eta) \|\eta\|^2 + \frac{2\sigma_{es} \lambda_{\max}(P_\eta) \|\eta\|}{\omega_o^3} \tag{34}$$

For $V(\eta)$, there exists $\lambda_{\min}(P_\eta) \|\eta\|^2 \leq V(\eta) \leq \lambda_{\max}(P_\eta) \|\eta\|^2$, i.e.,

$$\frac{V(\eta)}{\lambda_{\max}(P_\eta)} \leq \|\eta\|^2 \leq \frac{V(\eta)}{\lambda_{\min}(P_\eta)} \tag{35}$$

Substituting (35) into (34) yields

$$\dot{V}(\eta) \leq -\omega_o \frac{\lambda_{\min}(Q_\eta)}{\lambda_{\max}(P_\eta)} V(\eta) + \frac{2\sigma_{es} \lambda_{\max}(P_\eta)}{\omega_o^3 \sqrt{\lambda_{\min}(P_\eta)}} \sqrt{V(\eta)} \tag{36}$$

Letting $W = \sqrt{V(\eta)}$, it obtains that $\dot{W} = \frac{\dot{V}(\eta)}{2\sqrt{V(\eta)}}$. Substituting it into (36) yields

$$\dot{W} \leq -\omega_o \frac{\lambda_{\min}(Q_\eta)}{2\lambda_{\max}(P_\eta)} W + \frac{\sigma_{es}\lambda_{\max}(P_\eta)}{\omega_o^3 \sqrt{\lambda_{\min}(P_\eta)}} \tag{37}$$

According to Gronwall–Bellman inequality [40], it follows from (37) that

$$W \leq - \left(\frac{2\sigma_{es}\lambda_{\max}^2(P_\eta)}{\omega_o^4 \sqrt{\lambda_{\min}(P_\eta)}\lambda_{\min}(Q_\eta)} - W(T_0) \right) \cdot e^{-\omega_o \frac{\lambda_{\min}(Q_\eta)}{2\lambda_{\max}(P_\eta)}(T-T_0)} + \frac{2\sigma_{es}\lambda_{\max}^2(P_\eta)}{\omega_o^4 \sqrt{\lambda_{\min}(P_\eta)}\lambda_{\min}(Q_\eta)} \tag{38}$$

Combining (35) and (38), it is then obtained that

$$\|\eta\| \leq \frac{\sqrt{V(\eta)}}{\sqrt{\lambda_{\min}(P_\eta)}} \leq \frac{2\sigma_{es}\lambda_{\max}^2(P_\eta)}{\omega_o^4 \lambda_{\min}(P_\eta)\lambda_{\min}(Q_\eta)} = \frac{M_e}{\omega_o^4}, \quad (T \rightarrow \infty) \tag{39}$$

where $M_e = \frac{2\sigma_{es}\lambda_{\max}^2(P_\eta)}{\lambda_{\min}(P_\eta)\lambda_{\min}(Q_\eta)} > 0$. Since P_η and Q_η are both irrelevant to ω_o , it follows from (39) that

$$\lim_{\omega_o \rightarrow \infty, T \rightarrow \infty} \|\eta\| = 0 \tag{40}$$

By noticing $\eta_i = \frac{e_{si}}{\omega_{oi}} (i = 1, 2, 3)$, it obtains

$$\lim_{\omega_o \rightarrow \infty, T \rightarrow \infty} \|e_s\| = 0 \tag{41}$$

which means that the estimation error of the LESO can be made arbitrarily small by increasing the value of ω_o . This completes the proof. \square

Theorem 2. Consider the cascade TORA system (5) and (6) in the presence of unknown lumped disturbance d_τ . Design the controller as (27) with (13) and the LESO as (21). If the control gain is selected satisfying $k_1 > \frac{1}{2}$, then all the state variables remain bounded, and the system is stabilized at the target position, i.e.,

$$\lim_{t \rightarrow \infty} [\xi_1 \quad \xi_2 \quad y_1 \quad y_2]^\top = [0 \quad 0 \quad 0 \quad 0]^\top \tag{42}$$

Proof. First of all, the stability of system (20) is proven. Substituting (27) into (26) yields

$$\dot{V}_2 = -k_1 z_2^2 + z_2(z_3 - \hat{z}_3) = -k_1 z_2^2 + z_2 e_{s3} \tag{43}$$

Using Young’s inequality [41], it obtains

$$\dot{V}_2 \leq -k_1 z_2^2 + \frac{1}{2} z_2^2 + \frac{1}{2} e_{s3}^2 = -\left(k_1 - \frac{1}{2}\right) z_2^2 + \frac{1}{2} e_{s3}^2 \tag{44}$$

According to Theorem 1, noting that $\lim_{T \rightarrow \infty} \|e_s\| = 0$, if the control gain is selected satisfying $k_1 > \frac{1}{2}$, then $\dot{V}_2 \leq 0$, which leads to $\lim_{T \rightarrow \infty} z_2 = 0$. Employing LaSalle’s invariance principle [40], it is straightforward to obtain

$$\lim_{T \rightarrow \infty} [z_1 \quad z_2]^\top = [0 \quad 0]^\top \Rightarrow \lim_{T \rightarrow \infty} [e_1 \quad e_2]^\top = [0 \quad 0]^\top \tag{45}$$

Then, the stability of the subsystem (17) is analyzed. Applying (45), it assumes that $e_1 = 0$, then the subsystem (17) becomes

$$\begin{cases} \dot{\zeta}_1 = \zeta_2 \\ \dot{\zeta}_2 = -\zeta_1 + \varepsilon \sin y_{1d} \end{cases} \quad (46)$$

Note that the control Lyapunov function defined in (11) is

$$V_1 = \frac{1}{2}\zeta_1^2 + \frac{1}{2}\zeta_2^2 \quad (47)$$

Taking the time derivative of (47) along (46) and using (13) yields

$$\dot{V}_1 = -\zeta_2 \varepsilon \sin[\tanh(\alpha \zeta_2)] \leq 0 \quad (48)$$

where $\varepsilon > 0, \alpha > 0$, and the following properties of a generalized hyperbolic tangent function $y = \tanh(s)$ have been utilized.

$$\begin{cases} y \in (-1, 1) \\ \tanh(0) = 0 \\ s \cdot \tanh(s) \geq 0 \end{cases} \quad (49)$$

It follows from (48) that the closed-loop subsystem (46) under (13) is stable in the sense of Lyapunov, and all the state variables are bounded, i.e.,

$$V_1 \leq V_1(0) \in \mathcal{L}_\infty \Rightarrow \zeta_1, \zeta_2, y_{1d} \in \mathcal{L}_\infty \quad (50)$$

However, there is no guarantee that the state variables converge to zeros as V_1 is negative semi-definite.

To further prove the asymptotic convergence of the state variables, define the following invariant set

$$\Omega = \{(\zeta_1, \zeta_2) | V_1 \leq V_1(0)\} \quad (51)$$

Let Ω_M be the largest invariant set contained in Ω :

$$\Omega_M = \{(\zeta_1, \zeta_2) | \dot{V}_1 = 0\} \quad (52)$$

When $\dot{V}_1 = 0$, it follows from (48) that

$$\zeta_2 = 0 \Rightarrow \dot{\zeta}_2 = 0 \quad (53)$$

Further, substituting (53) into (13) and (46) yields

$$\dot{\zeta}_1 = 0, y_{1d} = 0 \Rightarrow \zeta_1 = 0 \quad (54)$$

As the set Ω_M is only made up of one point, according to LaSalle's invariance theorem, it concludes that the subsystem (17) is globally asymptotically stable at the origin, i.e.,

$$\lim_{T \rightarrow \infty} [\zeta_1 \quad \zeta_2]^\top = [0 \quad 0]^\top \quad (55)$$

Finally, it needs to analyze the convergence of the entire cascade system consisting of (17) and (18). Based on the above stability analysis, it is known that both the subsystem (17) and the subsystem (18) are globally asymptotically stable at the origin. Moreover, the right side of (17) is globally Lipschitz and bounded. By invoking Theorem 6.2 in [42], it concludes that the entire system is asymptotically stable at the equilibrium point, i.e.,

$$\lim_{T \rightarrow \infty} [\zeta_1 \quad \zeta_2 \quad e_1 \quad e_2]^\top = [0 \quad 0 \quad 0 \quad 0]^\top \quad (56)$$

which, by utilizing (14), is equivalent to

$$\lim_{T \rightarrow \infty} [\xi_1 \quad \xi_2 \quad y_1 \quad y_2]^\top = [0 \quad 0 \quad 0 \quad 0]^\top \quad (57)$$

Therefore, the control objective of the TORA system is realized and the proof of the Theorem 2 is completed. \square

5. Simulation Results

In this section, the effectiveness of the proposed control scheme is validated by numerical simulations in the MATLAB/Simulink platform. Moreover, the superior control performance of the devised controller is discussed by a series of comparison results with the sliding mode (SMC) controller proposed in [35].

During the simulation, the system parameter of the dimensionless model (3) is set as $\varepsilon = 0.2$. By trial and error, the gains of the proposed controller in (13) and (27) are chosen as $\alpha = 2.4, k_1 = 3$. The bandwidth of the LESO in (21) is $\omega_0 = 10$, and the gains of the LESO are obtained from (23) as $\beta_1 = 30, \beta_2 = 300, \beta_3 = 1000$. To ensure fair comparison, the control parameters of the comparative controller are chosen as the same as [35].

5.1. Case 1: Robustness to Continuous Disturbance

First of all, without loss of generality, the following continuous disturbance is imposed on the system, and the initial state of the system is set to be $[\chi \quad \dot{\chi} \quad \theta \quad \dot{\theta}]^\top = [1 \quad 0 \quad 0 \quad 0]^\top$.

$$d_\tau = \frac{10 \sin t}{(10 + 0.5t^2)} \quad (58)$$

The simulation results of the TORA system under the two controllers are depicted in Figures 3–5, which record the curves of the dimensionless trolley displacement, the ball rotational angle, and the dimensionless control input, respectively.

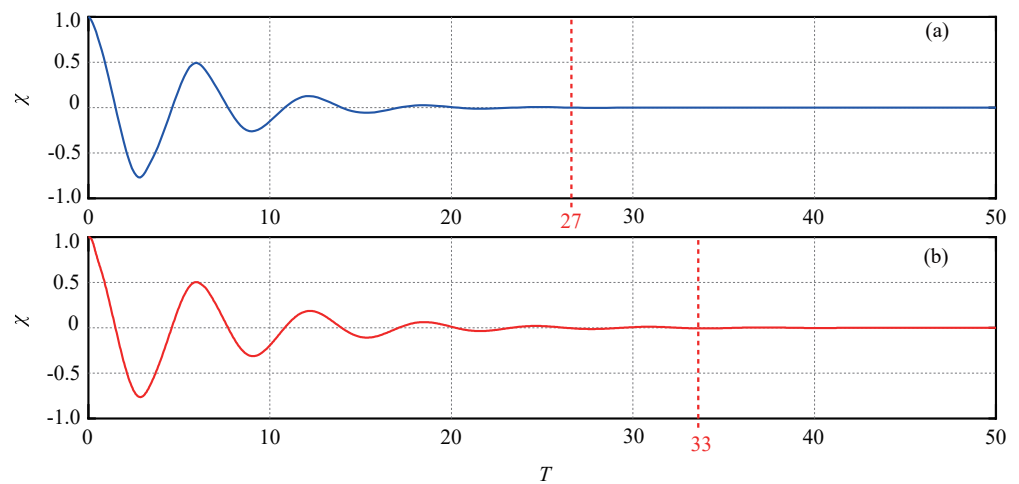


Figure 3. Curves of the dimensionless trolley displacement with a continuous disturbance [(a) Proposed method; (b) Method in [35]].

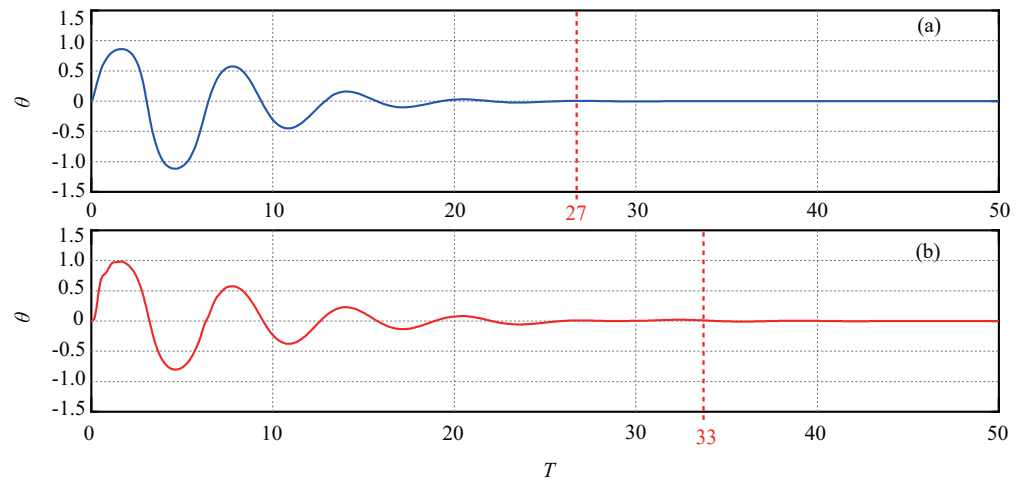


Figure 4. Curves of the dimensionless ball rotational angle with a continuous disturbance [(a) Proposed method; (b) Method in [35]].

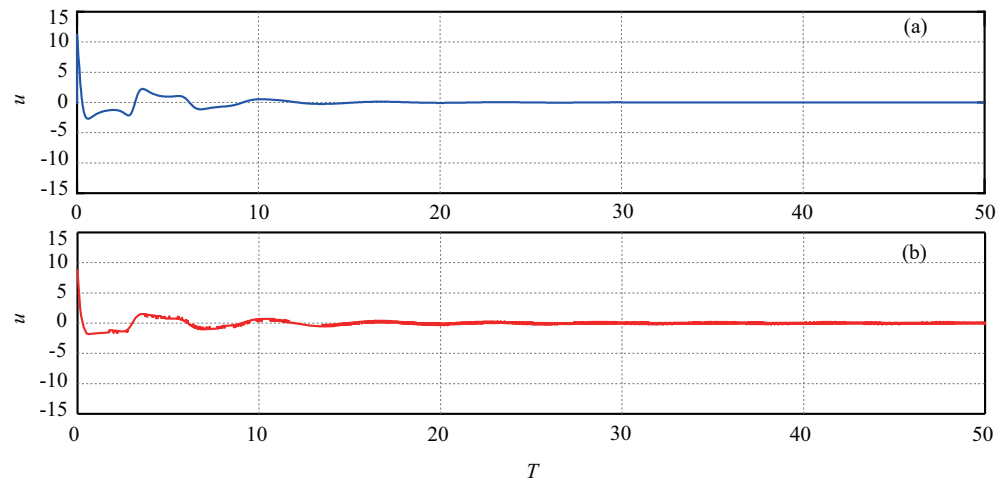


Figure 5. Curves of the dimensionless control input with a continuous disturbance [(a) Proposed method; (b) Method in [35]].

From Figures 3–5, it is observed that the trolley and the ball of the TORA system under the two controllers are stabilized at the equilibrium point. However, from Figures 3 and 4, we find that the settling time the proposed method, which is about 27, is much shorter than that (about 33) of the SMC controller in [35]. In addition, from Figure 5, it can be seen that there exists a serious chattering phenomenon in the SMC controller. In contrast, the controller proposed in this paper generates a continuous and smooth control input signal. These results demonstrate that the proposed control scheme achieves a faster and smoother control performance in the presence of continuous disturbance.

5.2. Case 2: Robustness Test to Different Disturbances

To further examine the robustness of the controllers to different disturbances, two different disturbances are imposed on the TORA system. The first one is a pulse with an amplitude of 3, which is added between the interval 6 and 6.2. Another one is a sinusoid disturbance with an amplitude of 3, which is added from 20 to 30. The initial state of the system is selected as $[\chi \ \dot{\chi} \ \theta \ \dot{\theta}]^T = [0 \ 0 \ 0 \ 0]^T$.

The simulation results of the TORA system under the two controllers are shown in Figures 6–8. It can be seen from Figures 6 and 7 that the states of the TORA system are affected by the external disturbances and deviate from the equilibrium position. However, soon, both the two controllers can attenuate the disturbances and be re-stabilize the system at the equilibrium point. However, by comparing the results in Figures 6 and 7, it is

found that the resettling time and the deviation magnitudes of the trolley displacement and the ball rotational angle with the proposed controller are smaller than those of the SMC method in [35]. In addition, from Figure 8, it is also seen that there exists a serious chattering phenomenon in the SMC controller, while the control input of the proposed controller is continuous and smooth. This group of simulation results demonstrates that the proposed control scheme achieves stronger and smoother robustness to external disturbances.

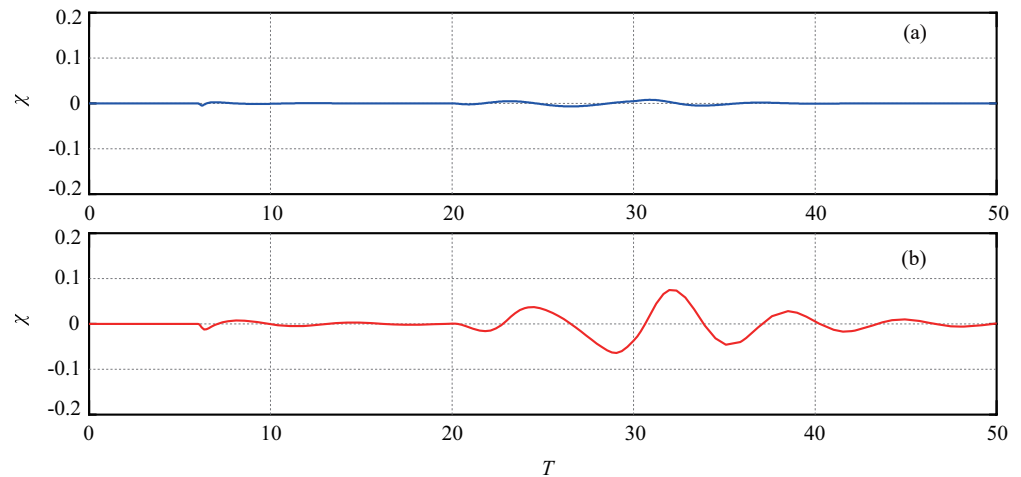


Figure 6. Robustness test results of the dimensionless trolley displacement under different external disturbances [(a) Proposed method; (b) Method in [35]].

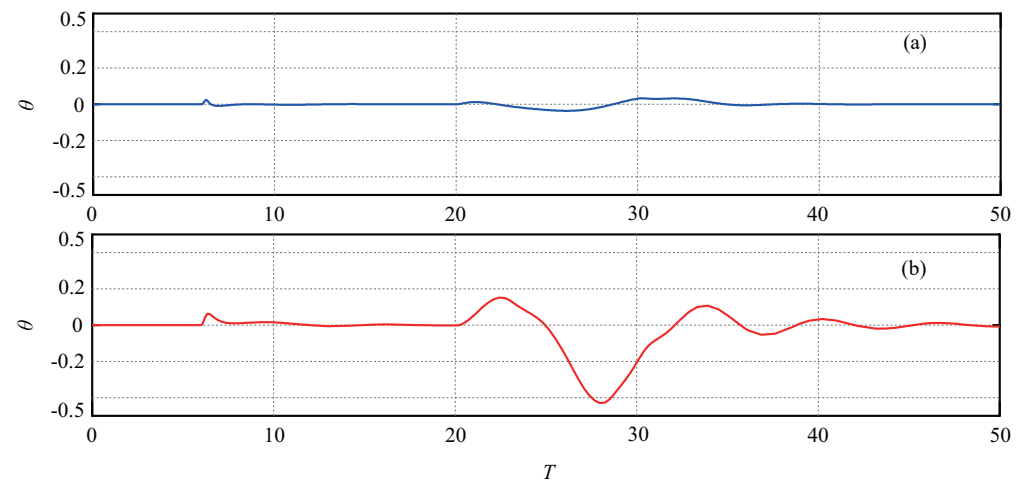


Figure 7. Robustness test results of the ball rotational angle under different external disturbances [(a) Proposed method; (b) Method in [35]].

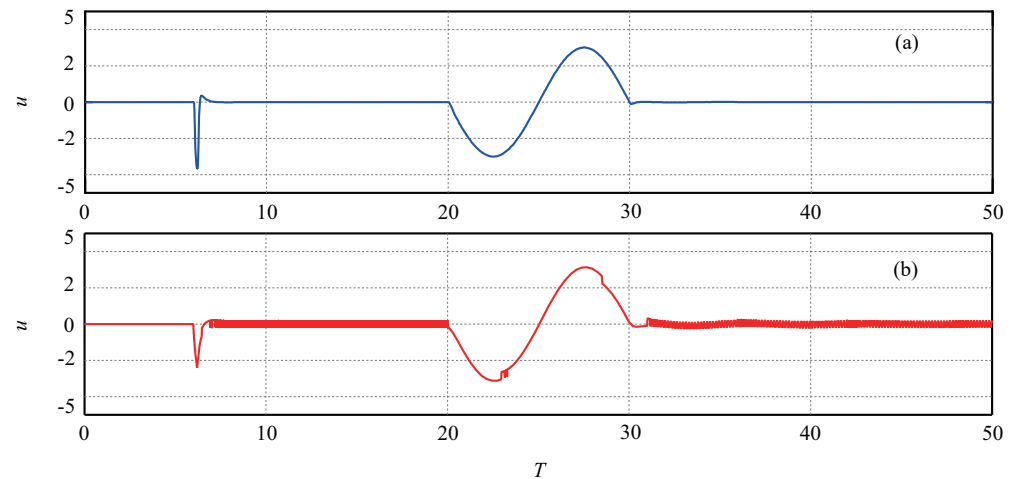


Figure 8. Robustness test results of the dimensionless control input [(a) Proposed method; (b) Method in [35]].

5.3. Estimation Performance of LESO

Finally, the estimation performance of the proposed LESO to the disturbances in the previous two cases are examined. To facilitate the analysis, the estimation error of the LESO is redefined as

$$\tilde{d}_n = d_n - \hat{d}_n \tag{59}$$

The obtained results of the two groups are shown in Figures 9 and 10, respectively. From these figures, it can be observed that as the time approaches infinity, the estimation errors approach zeros, and the proposed LESO can accurately estimate the uncertain disturbances. These simulation results demonstrate that the proposed LESO achieves a satisfactory estimation performance.

It should be noted that the parameters of the LESO are selected by regulating the bandwidth w_o according to (23). Generally speaking, increasing the bandwidth w_o would obtain a fast and good observation ability of the LESO but will result in a peaking phenomenon or serious oscillation. Therefore, a good w_o should be carefully selected by trial and error.

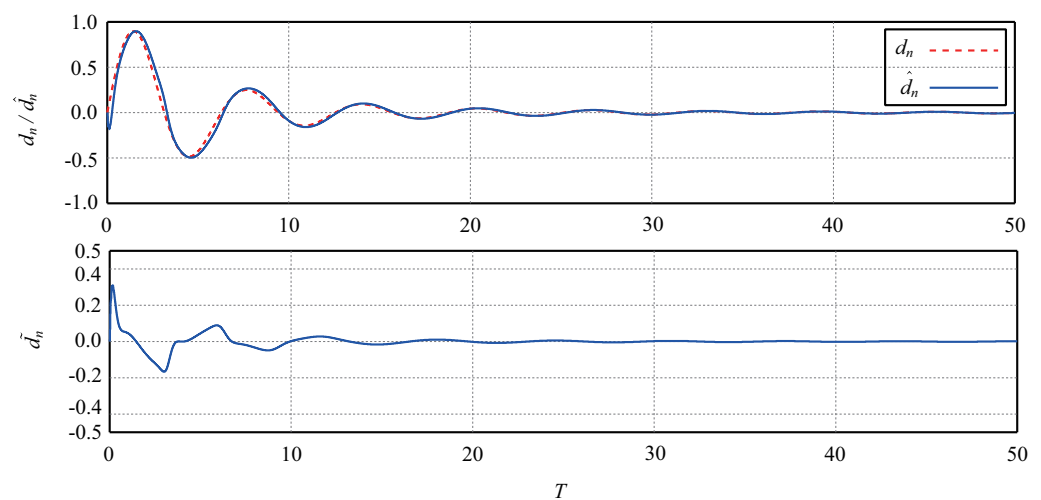


Figure 9. Estimation performance of LESO to the disturbance in Case 1.

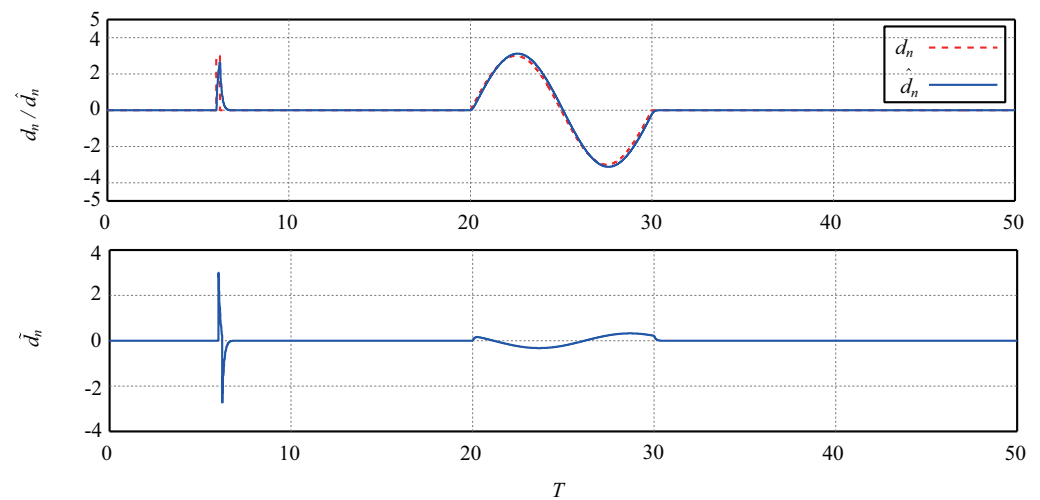


Figure 10. Estimation performance of LESO to the disturbance in Case 2.

6. Conclusions

This paper has proposed a nonlinear continuous robust control approach for the stabilization of underactuated TORA systems with unknown matched disturbances. The proposed control approach consists of backstepping virtual control law, a LESO, and a nonlinear state feedback control law. The proposed control algorithm can estimate and compensate the unknown disturbances in real-time, ensuring strong robustness to disturbances. In addition, it is capable of generating continuous control signals. The convergence and stability of the entire control system are rigorously guaranteed by Lyapunov theory and LaSalle's invariance principle. Simulation results with comparisons to the existing method show that the proposed approach achieves a better control performance, including shorter settling time, and smoother and stronger robustness to unknown disturbances.

It is worth noticing that only matched disturbances are taken in account in this paper. As stated in [17], for underactuated TORA systems with both matched and mismatched disturbances, there does not exist a feedback controller that can asymptotically stabilize all the state variables at the origin simultaneously. Therefore, the stabilization of TORA systems in the presence of matched and mismatched disturbances is still very challenging and needs to be further investigated in our future work.

Author Contributions: Conceptualization, C.P. and Y.W.; methodology, C.C.; software, Y.W.; validation, C.P., Y.W. and J.X.; formal analysis, Z.L.; investigation, C.P.; resources, C.P.; data curation, Y.W.; writing—original draft preparation, C.C.; writing—review and editing, C.P. and J.X.; visualization, Z.L.; supervision, C.P.; project administration, C.P. and J.X.; funding acquisition, C.P. and J.X. All authors have read and agreed to the published version of the manuscript.

Funding: This work is supported in part by (i) National Natural Science Foundation of China (Grant No. 62173138); (ii) Guangdong Basic and Applied Basic Research Foundation (Grant Nos. 2020A1515011082 and 2019A1515010955); (iii) Scientific Research Fund of Hunan Provincial Education Department (Grant Nos. 20A186 and 21C0329); (iv) Hunan Provincial Natural Science Foundation of China (Grant No. 2022JJ30263).

Institutional Review Board Statement: Not applicable.

Informed Consent Statement: Not applicable.

Data Availability Statement: Not applicable.

Conflicts of Interest: The authors declare no conflict of interest.

References

1. He, B.; Wang, S.; Liu, Y.J. Underactuated robotics: A review. *Int. J. Adv. Robot. Syst.* **2019**, *16*, 1729881419862164. [[CrossRef](#)]
2. Ouyang, H.; Tian, Z.; Yu, L.; Zhang, G. Partial enhanced-coupling control approach for trajectory tracking and swing rejection in tower cranes with double-pendulum effect. *Mech. Syst. Signal Process.* **2021**, *156*, 107613. [[CrossRef](#)]
3. Yang, T.; Sun, N.; Fang, Y. Neuroadaptive control for complicated underactuated systems with simultaneous output and velocity constraints exerted on both actuated and unactuated states. *IEEE Trans. Neural Netw. Learn. Syst.* **2021**. [[CrossRef](#)] [[PubMed](#)]
4. Yang, T.; Chen, H.; Sun, N.; Fang, Y. Adaptive neural network output feedback control of uncertain underactuated systems with actuated and unactuated state constraints. *IEEE Trans. Syst. Man Cybern. Syst.* **2021**. [[CrossRef](#)]
5. Yang, T.; Sun, N.; Fang, Y. Adaptive fuzzy control for a class of MIMO underactuated systems with plant uncertainties and actuator deadzones: Design and experiments. *IEEE Trans. Cybern.* **2021**. [[CrossRef](#)]
6. Chen, S.; Wang, Y.; Zhang, P.; Su, C.Y. Continuous control strategy of planar 3-linkage underactuated manipulator based on broad neural network. *Actuators* **2021**, *10*, 249. [[CrossRef](#)]
7. Robert, T.B.; Dennis, S.B.; Vincent, T.C. A benchmark problem for nonlinear control design. *Int. J. Robust Nonlinear Control* **1998**, *8*, 307–310.
8. Fradkov, A.; Tomchina, O.; Tomchin, D. Controlled passage through resonance in mechanical systems. *J. Sound Vib.* **2011**, *330*, 1065–1073. [[CrossRef](#)]
9. Sun, N.; Wu, Y.M.; Fang, Y.C.; Chen, H. Nonlinear stabilization control of multiple-RTAC systems subject to amplitude-restricted actuating torques using only angular position feedback. *IEEE Trans. Ind. Electron.* **2017**, *64*, 3084–3094. [[CrossRef](#)]
10. Zhang, Y.; Li, L.Y.; Cheng, B.W.; Zhang, X. An active mass damper using rotating actuator for structural vibration control. *Adv. Mech. Eng.* **2016**, *8*, 1687814016657730. [[CrossRef](#)]
11. Shah, S.A.A.; Gao, B.; Ahmed, N.; Liu, C. Advanced robust control techniques for the stabilization of translational oscillator with rotational actuator based barge-type OFWT. *Proc. Inst. Mech. Eng. Part M J. Eng. Marit. Environ.* **2021**, *235*, 327–343. [[CrossRef](#)]
12. He, M.E.; Hu, Y.Q.; Zhang, Y. Optimization design of tuned mass damper for vibration suppression of a barge-type offshore floating wind turbine. *Proc. Inst. Mech. Eng. Part M J. Eng. Marit. Environ.* **2017**, *231*, 302–315. [[CrossRef](#)]
13. Wu, Y.; Sun, N.; Fang, Y.; Liang, D. An increased nonlinear coupling motion controller for underactuated Multi-TORA systems: Theoretical design and hardware experimentation. *IEEE Trans. Syst. Man Cybern. Syst.* **2019**, *49*, 1186–1193. [[CrossRef](#)]
14. Pan, C.; Cui, C.; Zhou, L.; Xiong, P.; Li, Z. A model-free output feedback control approach for the stabilization of underactuated TORA system with input saturation. *Actuators* **2021**, *11*, 97. [[CrossRef](#)]
15. Pertres, Z.B.; Aranyi, P.; Korondi, P.; Hashimoto, H. Trajectory tracking by TP model transformation: Case study of a benchmark problem. *IEEE Trans. Ind. Electron.* **2007**, *54*, 1654. [[CrossRef](#)]
16. Quan, Q.; Cai, K.Y. Additive-state-decomposition-based tracking control for benchmark. *J. Sound Vib.* **2013**, *332*, 4829–4841. [[CrossRef](#)]
17. Sun, N.; Wu, Y.; Fang, Y.; Chen, H.; Lu, B. Nonlinear continuous global stabilization control for underactuated RTAC systems: Design, analysis, and experimentation. *IEEE/ASME Trans. Mechatron.* **2017**, *22*, 1104–1115. [[CrossRef](#)]
18. Jankovic, M.; Fontaine, D.; Kokotović, P.V. TORA example: Cascade- and passivity-based control designs. *IEEE Trans. Control. Syst. Technol.* **1996**, *4*, 292–297. [[CrossRef](#)]
19. Jiang, Z.P.; Kanellakopoulos, I. Global output feedback tracking for a benchmark nonlinear system. *IEEE Trans. Autom. Control* **2000**, *45*, 1023–1027. [[CrossRef](#)]
20. Wu, X.Q.; Xu, K.X.; Ma, M.; Ke, L.T. Output feedback control for an underactuated benchmark system with bounded torques. *Asian J. Control* **2020**, *23*, 1466–1475. [[CrossRef](#)]
21. Avis, J.M.; Nersesov, S.G.; Nathan, R. A comparison study of nonlinear control techniques for the RTAC system. *Nonlinear Anal. Real World Appl.* **2010**, *11*, 2647–2658. [[CrossRef](#)]
22. He, S.M.; Ji, H.B.; Yang, K.H. Semi-global output feedback tracking to reference system with input for a benchmark nonlinear system. *Asian J. Control* **2019**, *21*, 749–758. [[CrossRef](#)]
23. Gao, B.T. Dynamic modeling and energy-based control design of TORA. *Acta Autom. Sin.* **2008**, *34*, 1221–1224. (In Chinese with an English Abstract) [[CrossRef](#)]
24. Wu, X.Q.; Gu, M.M. Adaptive control of the TORA system with partial state constraint. *Trans. Inst. Meas. Control* **2019**, *41*, 1172–1177. [[CrossRef](#)]
25. Burg, T.; Dawson, D. Additional notes on the TORA example: A filtering approach to eliminate velocity measurements. *IEEE Trans. Control Syst. Technol.* **1997**, *5*, 520–523. [[CrossRef](#)]
26. Escobar, G.; Ortega, R.; Sira-Ramrez, H. Output-feedback global stabilization of a nonlinear benchmark system using a saturated passivity-based controller. *IEEE Trans. Control Syst. Technol.* **1999**, *7*, 289–293. [[CrossRef](#)]
27. Wu, X.Q.; Xu, K.X.; Zhang, Y.B. Output-based feedback control of underactuated TORA systems by bounded inputs. *Acta Autom. Sin.* **2020**, *46*, 200–204. (In Chinese with an English Abstract)
28. Gao, B.T.; Jia, Z.Y.; Chen, H.J.; Zhang, X. Dynamic modeling and backstepping control of TORA. *Control Decis.* **2007**, *22*, 1284–1288. (In Chinese with an English Abstract)
29. Liu, D.T.; Guo, W.P. Nonlinear backstepping design for the underactuated TORA system. *J. Vibroeng.* **2014**, *16*, 552–559.
30. Guo, W.P.; Liu, D.T. Nonlinear dynamic surface control for the underactuated translational oscillator with rotating actuator system. *IEEE Access* **2019**, *7*, 11844–11853. [[CrossRef](#)]

31. Lee, C.H.; Chang, S.K. Experimental implementation of nonlinear TORA system and adaptive backstepping controller design. *Neural Comput. Appl.* **2012**, *21*, 785–800. [[CrossRef](#)]
32. She, J.; Zhang, A.; Lai, X.; Wu, M. Global stabilization of 2-DOF underactuated mechanical systems—an equivalent-input-disturbance approach. *Nonlinear Dyn.* **2012**, *69*, 495–509. [[CrossRef](#)]
33. Wu, T.B.; Gui, W.H.; Hu, D.; Du, C. Adaptive fuzzy sliding mode control for translational oscillator with rotating actuator: A fuzzy model. *IEEE Access* **2018**, *6*, 55861–55869. [[CrossRef](#)]
34. Hung, L.C.; Lin, H.P.; Chung, H.Y. Design of self-tuning fuzzy sliding mode control for TORA system. *Expert Syst. Appl.* **2007**, *32*, 201–212. [[CrossRef](#)]
35. Wu, X.Q.; Zhao, Y.J.; Xu, K.X. Nonlinear disturbance observer based sliding mode control for a benchmark system with uncertain disturbances. *ISA Trans.* **2021**, *110*, 63–70. [[CrossRef](#)] [[PubMed](#)]
36. Wu, X.Q.; Xu, K.X. Global sliding mode control for the underactuated translational oscillator with rotational actuator system. *Proc. Inst. Mech. Eng. Part I J. Syst. Control Eng.* **2021**, *235*, 540–549.
37. Han, J. From PID to active disturbance rejection control. *IEEE Trans. Ind. Electron.* **2009**, *56*, 900–906. [[CrossRef](#)]
38. Wang, S.; Li, S.; Su, J.; Li, J.; Zhang, L. Extended state observer-based nonsingular terminal sliding mode controller for a DC-DC buck converter with disturbances: Theoretical analysis and experimental verification. *Int. J. Control* **2022**. [[CrossRef](#)]
39. Gao, Z. Scaling and bandwidth-parameterization based controller tuning. In Proceedings of the 2003 American Control Conference, Denver, CO, USA, 4–6 June 2003.
40. Khalil, H.K. *Nonlinear Systems*, 3rd ed.; Prentice Hall: Hoboken, NJ, USA, 2002.
41. Cunningham, F., Jr.; Grossman, N. On Young's Inequality. *Am. Math. Mon.* **1971**, *78*, 781–783. [[CrossRef](#)]
42. Sussmann, H.J.; Kokotovic, P.V. The peaking phenomenon and the global stabilization of nonlinear systems. *IEEE Trans. Autom. Control* **1991**, *36*, 424–440. [[CrossRef](#)]